

High intrinsic noise and absence of hysteresis in superconducting quantum interference devices with large Steward-McCumber parameter

Jia Zeng, Yi Zhang, Michael Mück, Hans-Joachim Krause, Alex I. Braginski, Xiangyan Kong, Xiaoming Xie, Andreas Offenhäusser, and Mianheng Jiang

Citation: [Applied Physics Letters](#) **103**, 042601 (2013); doi: 10.1063/1.4816730

View online: <http://dx.doi.org/10.1063/1.4816730>

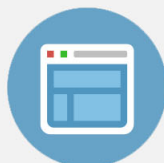
View Table of Contents: <http://scitation.aip.org/content/aip/journal/apl/103/4?ver=pdfcov>

Published by the [AIP Publishing](#)



Re-register for Table of Content Alerts

Create a profile.



Sign up today!



High intrinsic noise and absence of hysteresis in superconducting quantum interference devices with large Steward-McCumber parameter

Jia Zeng,^{1,2,3,4} Yi Zhang,^{2,3,a)} Michael Mück,⁵ Hans-Joachim Krause,^{2,3} Alex I. Braginski,² Xiangyan Kong,^{1,3} Xiaoming Xie,^{1,3} Andreas Offenhäusser,^{2,3} and Mianheng Jiang^{1,3}

¹State Key Laboratory of Functional Materials for Informatics, Shanghai Institute of Microsystem and Information Technology (SIMIT), Chinese Academy of Sciences (CAS), Shanghai 200050, China

²Peter Grünberg Institute (PGI-8), Forschungszentrum Jülich (FZJ), D-52425 Jülich, Germany

³Joint Research Laboratory on Superconductivity and Bioelectronics, Collaboration between CAS-Shanghai, Shanghai 200050, People's Republic of China and FZJ, D-52425 Jülich, Germany

⁴Graduate University of Chinese Academy of Sciences, Beijing 100049, China

⁵ez SQUID, Herborner Strasse 9, D-35764 Sinn, Germany

(Received 15 June 2013; accepted 10 July 2013; published online 24 July 2013)

We investigated niobium thin film superconducting quantum interference devices (SQUIDs) with large Steward-McCumber parameter ($\beta_c > 1$). No hysteresis was observed in the current-voltage (I - V) characteristics of the SQUIDs, even for $\beta_c \approx 17$. We attribute the absence of hysteresis to an excess voltage noise of the junctions which increases the SQUID intrinsic noise $\delta\Phi_s$. It can be represented by an effective noise temperature T^* of the SQUID which is higher than the bath temperature T . We simulated SQUID I - V characteristics using the measured device parameters and confirmed the absence of hysteresis. © 2013 AIP Publishing LLC. [<http://dx.doi.org/10.1063/1.4816730>]

There are two main noise sources in any direct-current (dc) superconducting quantum interference device (SQUID) system, the SQUID intrinsic noise $\delta\Phi_s$ and the noise $\delta\Phi_{\text{preamp}}$ produced by the preamplifier of the SQUID readout circuit. In order to obtain a low intrinsic noise, one usually designs the SQUID with a small McCumber parameter $\beta_c = 2\pi I_c C R_J^2 / \Phi_0 \leq 1$,¹ even $\leq 0.3 \sim 0.4$.² Here, I_c denotes the junction's critical current, C its self-capacitance, R_J the junction shunt resistance, and Φ_0 the magnetic flux quantum. In a conventional SQUID system, a readout electronics with flux modulation scheme (FMS)³ is employed to suppress the preamplifier noise. Without flux modulation, additional positive feedback circuitries can suppress $\delta\Phi_{\text{preamp}}$.⁴⁻⁶ Indeed, reading out the SQUID by a second SQUID usually yields the lowest preamplifier noise.⁷

The behavior of current-biased weakly damped junctions (i.e., $\beta_c > 1$) had been studied in several publications. One can infer from simulations by Tesche and Clarke⁸ that the value of β_c at which hysteresis appears in the quasi-static I - V characteristics is greater than one in the case of large thermal noise, while in the case of negligible noise, hysteresis appears at $\beta_c \approx 1$. For a quantitative description, they introduced the thermal rounding parameter $\Gamma = 2\pi k_B T / I_c \Phi_0$, where k_B denotes the Boltzmann constant, and T denotes the temperature. Tunnel junction simulations by Voss pointed out that the hysteresis can disappear for $\beta_c \geq 1$ while an excess voltage noise S_v appears across the junctions,⁹ thus rounding the I - V characteristics and preventing a hysteresis. In SQUID operation, although S_v will increase the SQUID intrinsic noise $\delta\Phi_s$,¹⁰ SQUIDs with large β_c exhibit a large voltage-to-flux transfer coefficient $\partial V / \partial \Phi$, which can conveniently be used to reduce $\delta\Phi_{\text{preamp}}$.¹¹⁻¹³ In the so-called direct readout scheme (DRS), the SQUID can be then

directly connected to an operational amplifier without the need for feedback circuitries to enhance $\partial V / \partial \Phi$, which simplifies the SQUID system substantially.

In this work, we measured a large number of SQUIDs in the current bias mode and determined their white noise, $\delta\Phi_s$, the flux-to-voltage transfer coefficient, $\partial V / \partial \Phi$, the critical current of the junctions, I_c , and the dynamic resistance at the working point, R_d , all at different values of β_c . Up to β_c approaching 20, we did not observe hysteresis but noted an increase in the intrinsic SQUID noise with β_c . The effective noise temperature $T^* > T_{\text{bath}} = 4.2$ K leads to an effective thermal rounding parameter Γ^* , which explains the absence of hysteresis.

In our experiments, we employed planar niobium-SQUID magnetometers with a pick-up-loop size of 5×5 mm² and a SQUID inductance of $L_s = 350$ pH.¹¹⁻¹³ The field-to-flux transfer coefficient $\partial B / \partial \Phi$ of these magnetometers reached 1.5 nT/ Φ_0 , approximately. We used two readout schemes to measure SQUID parameters and noise in flux-locked-loop (FLL): the traditional FMS using a step-up transformer, which reduces the effective voltage noise of the preamplifier to 0.08 nV/ $\sqrt{\text{Hz}}$ (at 100 kHz) when the primary coil of the transformer is shorted, and a simple DRS, without any feedback to enhance $\partial V / \partial \Phi$, i.e., the SQUID was directly connected to an operational amplifier used as a preamplifier (in our case AD 797). All SQUID chips were placed in a niobium shielding tube to perform the noise measurements.

It is difficult to determine β_c , which is a product of I_c , C , and R_J^2 experimentally, because the effective values of C and R_J cannot be measured easily for the high-frequency Josephson currents. We obtained a nominal β_c by using the measured value for I_c , the design value of the junction normal resistance, R_J (or R_J measured from I - V characteristics at large bias current), and a value of $C = 360$ fF, estimated from the junction's geometry. Generally, this capacitance

^{a)}Author to whom correspondence should be addressed. Electronic mail: y.zhang@fz-juelich.de

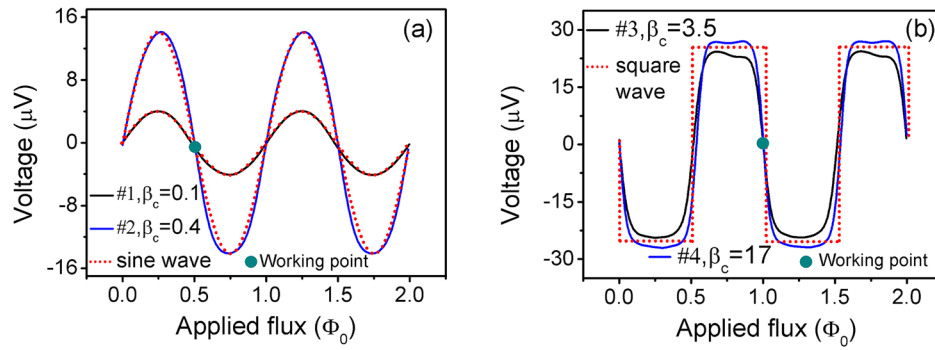


FIG. 1. Measured V - Φ curves of current-biased SQUIDs: (a) in the case of low nominal β_c of 0.1 (SQUID #1, $R_J = 5 \Omega$) and 0.4 (#2, $R_J = 10 \Omega$), and (b) in the case of high β_c of 3.5 (#3, $R_J = 30 \Omega$) and 17 (#4, $R_J = 65 \Omega$). Flux scale origin is arbitrary. The measured $2I_c$ of all SQUIDs was around $8 \mu\text{A}$. For $\beta_c < 1$, the shape of the V - Φ curves is quasi-sinusoidal but quasi-rectangular for $\beta_c > 1$, with no hysteresis observed. Sine and a square waves are traced with dotted lines to guide the eye.

consists of two parts: the junctions and the niobium traces of the counter electrode overlaying the SQUID washer. However, this capacitance may be influenced by the parasitic capacitances in the layout structures.¹⁴ To obtain a wide range of β_c values for a given SQUID geometry, R_J was varied while keeping constant I_c and C .

For meaningful statistics, we measured about 300 SQUID magnetometers with different β_c values. We used a DRS with a wide bandwidth (>1 MHz) to record the SQUID V - Φ and I - V curves and to derive $\partial V/\partial \Phi$ and R_d values. As β_c changes from $\beta_c \ll 1$ to larger values, the V - Φ curves change from a sine wave to a square wave, the latter indicating a $\beta_c \gg 1$. The measured V - Φ curves of SQUIDs with four typical values of β_c are shown in Figure 1.

The V - Φ curves shown for $\beta_c < 1$ (SQUID #1 and #2), are quasi-sinusoidal. With a β_c value increasing from 0.1 to 0.4, the voltage swing V_{swing} , the flux-to-voltage transfer coefficient $\partial V/\partial \Phi$, and R_d at working point obtained from the I - V characteristics, increased from $8 \mu\text{V}$ to $28 \mu\text{V}$, $30 \mu\text{V}/\Phi_0$ to $110 \mu\text{V}/\Phi_0$, and 3.5Ω to 10Ω , respectively.

The V - Φ curves of the two SQUIDs with $\beta_c > 1$ (SQUID #3 and #4), shown in Figure 1(b), are nearly rectangular without any hysteresis. In this range of β_c , V_{swing} increased only slightly, from $50 \mu\text{V}$ ($\beta_c = 3.5$) to $54 \mu\text{V}$ ($\beta_c = 17$) while both $\partial V/\partial \Phi$ and R_d increased further from $350 \mu\text{V}/\Phi_0$ to $600 \mu\text{V}/\Phi_0$ and 25Ω to 50Ω . All SQUID parameters measured by DRS are listed in Table I, including the noise analysis.

TABLE I. SQUID parameters measured by DRS.

SQUID No.		#1	#2	#3	#4
β_c^a	...	0.1	0.4	3.5	17
R_J^b	Ω	5	10	30	65
R_d^c	Ω	3.5	10	25	50
V_{swing}^d	μV	8	28	50	54
$\partial V/\partial \Phi^e$	$\mu\text{V}/\Phi_0$	30	110	350	600
$\delta\Phi_{\text{preamp}}^f$	$\mu\Phi_0/\sqrt{\text{Hz}}$	33	9.1	2.9	1.7
$\delta\Phi^f$	$\mu\Phi_0/\sqrt{\text{Hz}}$	33	9.3	4.2	7.2
$\delta\Phi_s^g$	$\mu\Phi_0/\sqrt{\text{Hz}}$...	1.9	3.0	7

^{a,b}The nominal value.

^cDerived from the I - V characteristics.

^{d,e}Obtained from traces of Figure 1.

^fMeasured SQUID system noise in FLL mode.

^gNot determined.

To verify that the measured system flux noise $\delta\Phi$ of SQUID #4 is dominated by $\delta\Phi_s$, the noise spectrum was also measured by FMS readout electronics. Noise levels of this SQUID were almost the same as shown in Figure 2.

The measured system noise $\delta\Phi$ listed in Table I is the sum of $\delta\Phi_s$ and $\delta\Phi_{\text{preamp}}$, i.e., $\delta\Phi = [\delta\Phi_s^2 + \delta\Phi_{\text{preamp}}^2]^{1/2}$. In our DRS, a commercial operational amplifier with a voltage noise $V_n \approx 1 \text{ nV}/\sqrt{\text{Hz}}$ ($>100 \text{ Hz}$) was used as preamplifier; its noise contribution can be expressed as $\delta\Phi_{\text{preamp}} \approx V_n/(\partial V/\partial \Phi)$.¹² When increasing β_c from 0.1 up to 17, $\partial V/\partial \Phi$ of SQUID increased from $30 \mu\text{V}/\Phi_0$ up to $600 \mu\text{V}/\Phi_0$, thus reducing $\delta\Phi_{\text{preamp}} \approx V_n/(\partial V/\partial \Phi)$ from about 33 to $1.7 \mu\Phi_0/\sqrt{\text{Hz}}$. Table I shows two limiting cases: $\delta\Phi_{\text{preamp}}$ dominates $\delta\Phi$ because of a small $\partial V/\partial \Phi$ of SQUID #1 and #2 while $\delta\Phi_s$ dominates $\delta\Phi$ due to a large β_c of SQUID #4. The minimal $\delta\Phi$ of $4.2 \mu\Phi_0/\sqrt{\text{Hz}}$ appears at $\beta_c \approx 3.5$ for SQUID #3. Here, both $\delta\Phi_s$ and $\delta\Phi_{\text{preamp}}$ contribute to $\delta\Phi$ with the same weight, i.e., $\delta\Phi_s \approx \delta\Phi_{\text{preamp}}$.

Voss⁹ noted that an excess voltage noise S_v across a tunnel junction is produced by random switching between the superconducting and nonzero voltage states in the case of $\beta_c > 0$. We interpret the increase of $\delta\Phi_s$ up to $7 \mu\Phi_0/\sqrt{\text{Hz}}$ by an increase in S_v of the junction with β_c . Indeed, both the Johnson noise and the random switching noise contribute to $\delta\Phi_s$, i.e., $\delta\Phi_s^2 = 2k_B T [L_s^2/R_J + 2R_d/(\partial V/\partial \Phi)^2] + S_v/(\partial V/\partial \Phi)$. Here, the Johnson noise contains two parts,¹⁵ a static term $2k_B T L_s^2/R_J$ and a dynamic term $4k_B T R_d/(\partial V/\partial \Phi)^2$. At $\beta_c \gg 1$, S_v dominates $\delta\Phi_s$.

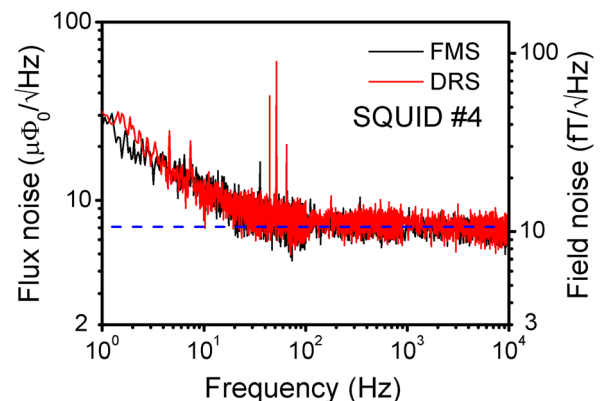


FIG. 2. Noise measurements of SQUID #4 with both DRS and FMS.

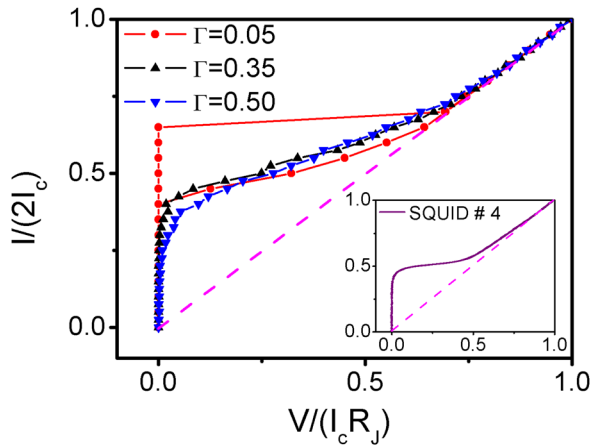


FIG. 3. Three simulated I - V characteristics of a symmetric SQUID with $\Gamma=0.05, 0.35, 0.5$ and $\beta_c=17$, $\beta_L=1$, at applied integer flux $\Phi=n\Phi_0$. The inset shows the measured I - V characteristic of SQUID #4, which agrees best with the simulation at $\Gamma=0.35$. Symbols V and I denote the time averaged dc voltage and bias current.

We introduce an effective noise temperature T^* , which is usually used to characterize amplifier noise, to rewrite the expression above: $\delta\Phi_s^2 = 2k_B (T + T^*) [L_s^2/R_J + 2R_d/(\partial V/\partial\Phi)^2]$. The value of $(T + T^*) \approx 30$ K is obtained for $\beta_c \approx 17$ (SQUID # 4). A $(T + T^*)$ of 30 K leads to the effective thermal rounding parameter, Γ^* , of 0.35, which is much larger than the value of $\Gamma=0.05$ ($T \approx 4.2$ K, $I_c = 4$ μ A) used in the simulations by Voss.⁹ This high Γ^* results in rounding of I - V characteristics thus causing the hysteresis to disappear. Figure 3 shows three simulated I - V characteristics with different Γ based on the model of a symmetric SQUID⁸ with $\beta_c=17$ and $\beta_L=2L_sI_c/\Phi_0 \approx 1$. For $\Gamma=0.05$, the I - V characteristic is obviously hysteretic. However, the hysteresis disappears at $\Gamma=0.35$ ($T=30$ K), which agrees with the measured I - V curve of SQUID #4 shown in the inset. At $\Gamma=0.5$, the rounding effect is even stronger.

To conclude, the V - Φ curves of dc SQUIDs can be generally described as quasi-sine waves when $\beta_c < 1$ and quasi-square waves, if $\beta_c > 1$. Indeed, three important SQUID

parameters, the intrinsic noise $\delta\Phi_s$, the voltage-to-flux transfer coefficient $\partial V/\partial\Phi$, and the dynamic resistance R_d , increase with increasing β_c . In our measurements, a hysteresis was not observed up to nominal $\beta_c \approx 17$. The absence of any hysteresis is explained by the large random switching noise, S_v , leading to high values of the effective thermal rounding parameter Γ^* and thus, a rounding of the SQUID I - V curve. Our simulations support this interpretation.

This work was supported by the “Strategic Priority Research Program (B)” of the Chinese Academy of Sciences (Grant No. XDB04010100).

- ¹J. Clarke, W. M. Goubau, and M. B. Ketchen, *J. Low Temp. Phys.* **25**, 99–144 (1976).
- ²M. Schmelz, R. Stolz, V. Zakosarenko, T. Schönau, S. Anders, L. Fritzsche, M. Mück, and H.-G. Meyer, *Supercond. Sci. Technol.* **24**, 065009 (2011).
- ³R. L. Forgacs and A. Warnick, *Rev. Sci. Instrum.* **38**, 214 (1967).
- ⁴D. Drung, R. Cantor, M. Peters, H. J. Scheer, and H. Koch, *Appl. Phys. Lett.* **57**, 406–408 (1990).
- ⁵H. Seppä, A. Ahonen, J. Knuutila, J. Simola, and V. Vilkmán, *IEEE Trans. Magn.* **27**, 2488–2490 (1991).
- ⁶X. Xie, Y. Zhang, H. Wang, Y. Wang, M. Mück, H. Dong, H.-J. Krause, A. I. Braginski, A. Offenhäusser, and M. Jiang, *Supercond. Sci. Technol.* **23**, 065016 (2010).
- ⁷F. C. Wellstood, C. Urbina, and J. Clarke, *Appl. Phys. Lett.* **50**, 772 (1987).
- ⁸C. D. Tesche and J. Clarke, *J. Low Temp. Phys.* **29**, 301–331 (1977).
- ⁹R. F. Voss, *J. Low Temp. Phys.* **42**, 151–163 (1981).
- ¹⁰D. Drung and W. Jutzi, *IEEE Trans. Magn.* **21**, 430–433 (1985).
- ¹¹Y. Zhang, C. Liu, M. Schmelz, H.-J. Krause, A. I. Braginski, R. Stolz, X. Xie, H.-G. Meyer, A. Offenhäusser, and M. Jiang, *Supercond. Sci. Technol.* **25**, 125007 (2012).
- ¹²C. Liu, Y. Zhang, M. Mück, H.-J. Krause, and A. I. Braginski, *Appl. Phys. Lett.* **101**, 222602 (2012).
- ¹³C. Liu, Y. Zhang, M. Mück, S. Zhang, H.-J. Krause, A. I. Braginski, G. Zhang, Y. Wang, X. Kong, X. Xie, A. Offenhäusser, and M. Jiang, *Supercond. Sci. Technol.* **26**, 065002 (2013).
- ¹⁴M. Schmelz, R. Stolz, V. Zakosarenko, T. Schönau, S. Anders, L. Fritzsche, M. Mück, M. Meyer and H.-G. Meyer, *Physica C* **482**, 27–32 (2012).
- ¹⁵R. Cantor, “DC SQUIDs: Design, Optimization and Practical Applications,” *SQUID Sensors: Fundamentals, Fabrication and Applications* (NATO ASI Series E Vol. 329), edited by H. Weinstock, Kluwer Academic Publishers, pp. 179–233 (1996).